FEM BASED PROCESS DESIGN FOR LASER FORMING OF DOUBLY CURVED SHAPES

Chao Liu and Y. Lawrence Yao
Department of Mechanical Engineering, Columbia University,
220 Mudd Bldg., MC 4703, New York, NY 10027

ABSTRACT

This study presents a finite element method (FEM) based three-dimensional laser forming process design methodology for thin plates to determine the laser scanning paths and heating conditions. The strain fields were first calculated via elastic large deformation FEM model. The laser scanning paths were chosen perpendicular to the averaged principal minimum strain direction. The ratios of in-plane and bending strain were calculated to help determine the heating conditions. A typical doubly curved shape, pillow shape, was studied and the overall methodology was validated by experiments.

INTRODUCTION

Significant progress has been made in analyzing and predicting laser forming processes of sheet metal. In order to advance the process further for realistic forming applications in an industrial setting it is necessary to consider process design, which is concerned with determination of laser scanning paths and heating condition given a desired shape to form.

A number of approaches have been attempted in the past few years in two-dimensional laser forming. Genetic algorithm based design (Shimizu, 1997; and Cheng and Yao, 2001) and response surface methodology based robust design (Liu and Yao, 2002) for cylindrical shapes and axis-symmetrical shapes have been proposed and validated in several cases numerically and experimentally. However, due to the geometry complexity of the doubly curved shapes, these methods are not appropriate for the general 3D process design.

In a series of reports, Ueda, et al. (1994a & b) addressed issues in the development of computer-aided process planning system for plate bending by line heating. In the first report, the concept of inherent strain was emphasized but its significance was not adequately argued or demonstrated. Scanning paths were determined based on FEM determined in-plane strain and heating condition determination was not addressed. This approach is not applicable to laser forming process design no consideration for the characteristic properties of laser forming process was given. In the second report, forming procedures of three simple curved shapes often encountered in shipyards were examined. The prediction was found to be in agreement with the real practice of skilled workers. However, the approach too heavily relied on a prior experience. Moreover, for the case when bending strain is relatively large, mechanical means such as a rolling machine was used to generate the bending strain, which is not suitable for an automatic laser forming process.

Edwardson, et al. (2001) and Watkins, et al. (2001) aimed to establish rules for positioning and sequencing scanning paths required for the 3D laser forming of a saddle shape from rectangular sheet material. Various scanning patterns were first postulated and then FEM modeled. However, the work too heavily relied on a prior experience in coming up with the patterns and may become even less effective when shapes to be formed become more complex. Furthermore, a constant scanning speed was assumed throughout an entire scanning pattern of a shape and this severely limits the realization of the full process capability of laser forming.

Cheng and Yao (2002) presented a methodology to design laser scanning paths and heating condition of laser forming for a general class of 3D shapes from thin sheet metal. The strain field was calculated by FEM. In determining laser scanning paths and heating condition, however, this method only considered the in-plane component of the total strain and therefore may incur larger errors when the bending component are not negligible. Liu, et al. (2002) proposed strategies for solving essentially the same process design problem as above. The strain field was determined based on differential geometry and an optimization approach. This method, however, concerned the middle surface only, again neglected the effect of bending strains across the thickness of a plate.

This study presents a FEM based 3D laser forming process design method for thin plates with consideration of the effect of bending strains. The strain field was calculated via elastic large deformation FEM model. The laser scanning paths were chosen perpendicular to the averaged principal minimum strain direction between top surface and middle surface. The ratios of in-plane and bending strain were calculated to help determine the heating condition. A typical doubly curved shape was studied and the overall methodology was validated by experiments.

PROBLEM DESCRIPTION

The flexural properties of a plate depend greatly upon its thickness in comparison with other dimensions. A thin plate has a ratio of $10<a/h<100$, where h is a plate thickness, a is a typical dimension of a plate (Ventsel and Krauthammer, 1994). In this study the ratios a/h of the desired shape is about 57, as opposed to about 123 in Cheng and Yao (2002) and about 90 in Liu, et al. (2002). As an extension to previous work, this study considered the effects of bending strains on the laser forming of a plate.

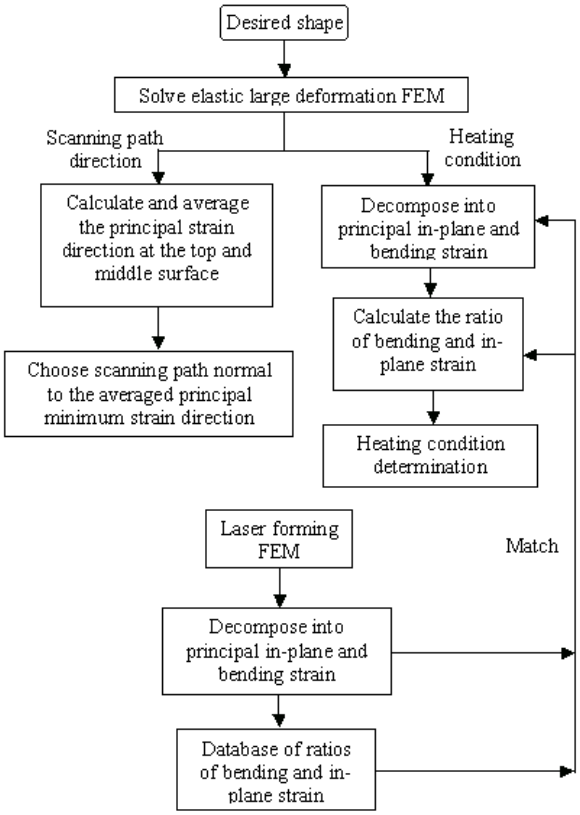

FIG. 1 FLOW CHART OF LASER FORMING PROCESS DESIGN.

The overall design strategy is outlined in Fig 1. First, a strain field is obtained by flattening a curved surface into a planar shape via FEM. After obtaining the strain field, the principal minimum strains and directions in both middle and top surface are calculated by solving the eigenvalues and eigenvectors of the strain tensor. Because, in the laser forming process, the highest compressive strains occur in the direction perpendicular to a scanning path, it is natural to place a laser path perpendicular to the principal minimum strain direction. In this study, scanning paths are chosen to be perpendicular to the averaged minimal principal strain directions between top and middle surface.

Different from forming a singly curved shape, forming a doubly curved shape requires not only bending strain (angular distortion), but also in-plane strain (stretching/contraction of the middle surface of a plate). Therefore at each material point in the plate, the principal minimum strain can be decomposed into in-plane strain and

bending strain. It is important to determine heating conditions (i.e., laser power *P* and scanning speed *V*) of a laser forming process such that not only the total strain at each point but also the ratio between the in-plane and bending strains are realized. This is possible because, although a strain field generated by the laser forming process has its own characteristics; such characteristics may vary even under the same line energy input level (i.e., the same *P/V* ratio) and therefore provide the possibility of matching the desired strains and ratio. In order to do so, a database of laser forming FEM results based on the simplest straight scan but under a variety of conditions and validated experimentally, is established to aid the heat condition determination.

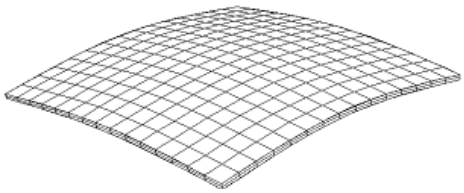

FIG. 2 A DOUBLY CURVED SHAPE (PILLOW SHAPE) TO BE LASER FORMED (80 BY 80 BY 1.4 MM).

A pillow shape, which is a doubly curved shape and has positive Gaussian curvatures over the entire surface, is chosen as the desired shape in this study. It is specified by a cubic-spline cross-section sweeping along a path of cubic-spline curve. The sweep surface is defined by: *S(x,y)=A(x)+B(y)*, where *x,y* $\in$[0,80] by [0,80] in mm, *A(x)* is defined by interior knots (0,0,0), (40,0,1.7), and (80,0,0) and *B(y)* defined by (0,0,0), (0,40,2.9) and (0,80,0). Note the adjacent sides of the pillow shape are not identical, with the one along the *y* direction curves slightly higher. The thickness of the plate is 1.4mm. Material is 1010 steel. The desired shape is shown in Fig. 2.

STRAIN FIELD ATTAINMENT

As indicated in the previous section, the first step in the laser forming process design is to determine the strain field required to form into the desired shape. The development of a strain field from one shape to another is primarily a geometrical problem and is independent of material properties, including both elastic and plastic properties. In fact, it has been shown that the strain field determination is independent of the Young's modules and details can be found in Cheng and Yao (2002). It was shown whether it is a soft (smaller Young's module value) or a hard (larger Young's modules value) material, the strain field remains the same. But the field depends on the Poison Ratio value which is a geometric parameter. Elastic FEM is therefore used instead of elastic/plastic FEM for this geometrical step since less material properties need to be specified in the elastic FEM. The large deformation model is employed for the following reasons. In the case of small deflection, the normal displacement component of the midplane (w_0) is small compared with the plate thickness *(h),* and thus the in-plane strain can be neglected. However, if the magnitude of deflection increases beyond a certain level ($w_0>0.3h$), these deflections are accompanied by stretching or contraction of the mid plane, and therefore cannot be neglected (Ventsel and Krauthammer, 1994). In this study, the ratio w_0/h reaches 3.3 and therefore large deformation FEM is necessary.

The governing relations for elastic large deformation of a thin plate are briefly summarized. It is assumed that the material of the plate is elastic, homogenous, and isotropic; the straight lines, initially normal to the middle surface before bending, remain straight and normal to the middle surface during the deformation and the length of such element is not altered. Deflection w_0 in the *z* (thickness) direction is assumed large relative to the thickness *h* of the plate and therefore membrane forces (N_x, N_y, and N_{xy}) become more pronounced. On the middle surface, the equilibrium equations are (Ventsel and Krauthammer, 1994)

$$\varepsilon_{xx}^0 = \frac{\partial u_0}{\partial x} + \frac{1}{2}\left(\frac{\partial w_0}{\partial x}\right)^2,\ \varepsilon_{yy}^0 = \frac{\partial v_0}{\partial x} + \frac{1}{2}\left(\frac{\partial w_0}{\partial y}\right)^2,$$

$$\gamma_{xy}^0 = \frac{\partial u_0}{\partial y} + \frac{\partial v_0}{\partial x} + \frac{\partial w_0}{\partial x}\frac{\partial w_0}{\partial y} \qquad (1)$$

where u_0, v_0, w_0 are the displacement components and $\varepsilon_{xx}^0, \varepsilon_{yy}^0$ and γ_{xy}^0 are the strains at the middle surface, respectively.

Eliminating the displace component u_0 and v_0

gives the compatibility equation:

$$\frac{\partial^2 \varepsilon_{xx}^0}{\partial y^2} + \frac{\partial^2 \varepsilon_{yy}^0}{\partial x^2} - \frac{\partial^2 \gamma_{xy}^0}{\partial x \partial y} = \left(\frac{\partial^2 w_0}{\partial x \partial y}\right)^2 - \frac{\partial^2 w_0}{\partial x^2}\frac{\partial^2 w_0}{\partial y^2} \qquad (2)$$

The constitutive relations for the large-deflection plate analysis follow Hook's law and can be expressed as

$$\frac{1}{Eh}\left[\frac{\partial^2}{\partial y^2}(N_x-\nu N_y)+\frac{\partial^2}{\partial x^2}(N_y-\nu N_x-2(1+\nu)\frac{\partial^2 N_{xy}}{\partial x\partial y}\right]$$
$$=\left(\frac{\partial^2 w_0}{\partial x\partial y}\right)^2-\frac{\partial^2 w_0}{\partial x^2}\frac{\partial^2 w_0}{\partial y^2} \quad (3)$$

where $\varepsilon^0_{xx}=\frac{1}{Eh}\left(N_x-\nu N_y\right)$, $\varepsilon^0_{yy}=\frac{1}{Eh}\left(N_y-\nu N_x\right)$, and $\gamma^0_{xy}=\frac{N_{xy}}{Gh}$; *E* and *G* are young's modulus and shear modulus, respectively, and ν is Poisson ratio.

The strains, membrane forces and displacement w_0 can be solved by the above set of equations, yielding two governing differential equations

$$\frac{\partial^4\varphi}{\partial x^4}+2\frac{\partial^4\varphi}{\partial x^2\partial y^2}+\frac{\partial^4\varphi}{\partial y^4}=h\left[\left(\frac{\partial^2 w_0}{\partial x\partial y}\right)^2-\frac{\partial^2 w_0}{\partial x^2}\frac{\partial^2 w_0}{\partial y^2}\right] \quad (4)$$

$$\frac{\partial^4 w_0}{\partial x^4}+2\frac{\partial^4 w_0}{\partial x^2\partial y^2}+\frac{\partial^4 w_0}{\partial y^4}=$$
$$\frac{1}{D'}\left[P'+\frac{\partial^2\varphi}{\partial y^2}\frac{\partial^2 w_0}{\partial x^2}+\frac{\partial^2\varphi}{\partial x^2}\frac{\partial^2 w_0}{\partial y^2}-2\frac{\partial^2\varphi}{\partial x\partial y}\frac{\partial^2 w_0}{\partial x\partial y}\right] \quad (5)$$

where $D'=\frac{h^3}{12(1-\nu^2)}$, $N_x=\frac{\partial^2\phi}{\partial y^2}$, $N_y=\frac{\partial^2\phi}{\partial x^2}$

$N_{xy}=-\frac{\partial^2\phi}{\partial x\partial y}$, $\varphi = \phi/E$ and *P'(x,y)* is lateral load in *z* direction *P(x,y)* divided by *E.*

Once a desired shape is given, that is, deflection w_0, and curvatures $\frac{\partial^2 w_0}{\partial x^2}$, $\frac{\partial^2 w_0}{\partial y^2}$, and $\frac{\partial^2 w_0}{\partial x\partial y}$ are known, φ and *P'* and in turn the in-plane strains ε^0_{xx}, ε^0_{yy}, and γ^0_{xy} can be calculated under appropriate boundary conditions and the calculation is independent of Young's modulus. However, equation (3) indicate that ε^0_{xx}, ε^0_{yy}, and γ^0_{xy} depend on Poisson ratio ν, which is a geometric parameter.

Under the thin plate assumption, the bending strain of deflection of a thin plate can be expressed as the following,

$$\varepsilon^1_{xx}=\varepsilon_{xx}-\varepsilon^0_{xx}=-z\frac{\partial^2 w_0}{\partial x^2}$$
$$\varepsilon^1_{yy}=\varepsilon_{yy}-\varepsilon^0_{yy}=-z\frac{\partial^2 w_0}{\partial y^2}$$
$$\gamma^1_{xy}=\gamma_{xy}-\gamma^0_{xy}=-z\frac{\partial^2 w_0}{\partial x\partial y} \quad (6)$$

where ε_{xx}, ε_{yy}, γ_{xy}, are total strains, and ε^1_{xx}, ε^1_{yy}, and γ^1_{xy} are bending strains. In equation (6), Therefore, the magnitude of bending strain is linearly proportional to the thickness *h* of the plate. From the concept of in-plane strain and equation (6) the strains at the middle surface can be taken as the in-plane strain. The FEM is implemented in ABAQUS.

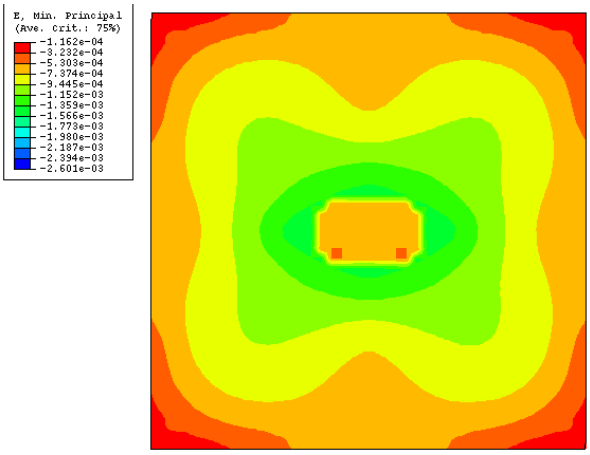

FIG. 3 MINIMUM PRINCIPAL STRAIN IN MIDDLE SURFACE OF THE PILLOW SHAPE (80 BY 80 BY 1.4MM).

Principal Strain Decomposition

From the FEM implementation, the strains are obtained in terms of tensor while as seen from the previous section only components in the *x* and *y* planes are concerned due to the thin plate assumption. They are determined as follows.

Given a strain tensor **E, E** can be expressed in terms of $\boldsymbol{\varepsilon_1 n_1 n_1^T}+\boldsymbol{\varepsilon_2 n_2 n_2^T}+\boldsymbol{\varepsilon_3 n_3 n_3^T}$ where principal strains $\boldsymbol{\varepsilon_1}$, $\boldsymbol{\varepsilon_2}$, and $\boldsymbol{\varepsilon_3}$ ($\varepsilon_1 \le \varepsilon_2 \le \varepsilon_3$) and the orientation of the principal strain, $\mathbf{n}_1$,$\mathbf{n}_2$, and $\mathbf{n}_3$ correspond to the eigenvalues and eigenvectors of the strain tensor **E** at that material point. Therefore $\boldsymbol{\varepsilon_1}$, $\boldsymbol{\varepsilon_2}$, and $\boldsymbol{\varepsilon_3}$, and $\mathbf{n}_1$, $\mathbf{n}_2$ and $\mathbf{n}_3$ can be obtained by solving the eigenvalue problem

$$\mathbf{En}=\boldsymbol{\varepsilon n} \quad (7)$$

where $\boldsymbol{\varepsilon}$ and **n** are principal strain and corresponding principal strain direction. Fig. 3 shows the color contour plot of the minimal principal strain (ε^0_1) distribution in the middle surface of the desired shape obtained from the FEM model.

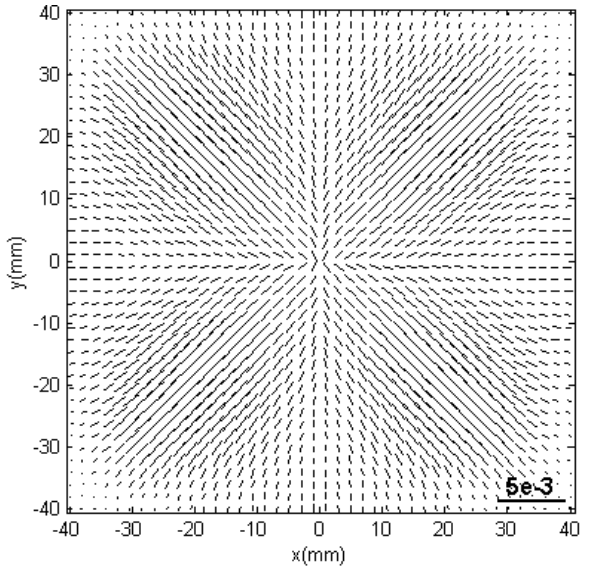

(a)

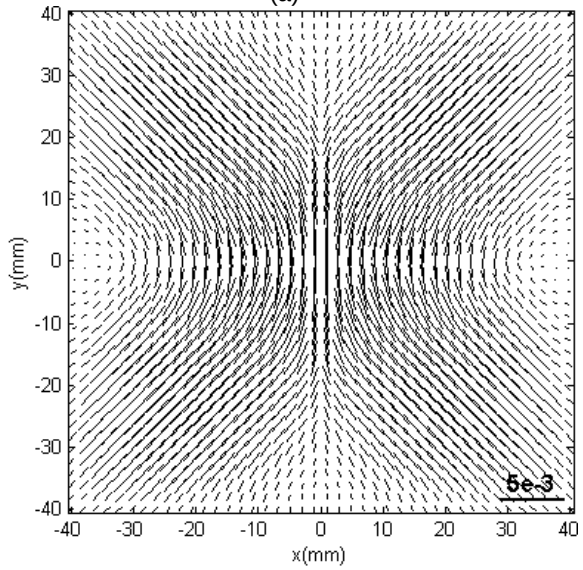

(b)

FIG. 4 VECTOR PLOTS OF MINIMUM PRINCIPAL STRAIN AT (A) MIDDLE SURFACE, AND (B) TOP SURFACE OF THE PILLOW SHAPE (LENGTH REPRESENTS STRAIN MAGNITURE AND ORIENTATION REPRESENTS STRAIN DIRECTION).

Fig. 4 (a) and (b) show the magnitude and orientation of principal minimum strain at the middle surface ($\varepsilon_1^0\ \mathbf{n}_1^0$) and top surface ($\boldsymbol{\varepsilon_1 n_1}$), respectively. The length of a bar in the plots represents the magnitude of the principal minimum strain. These strains represent the required strain field at these plans to be realized by a laser forming process. For thin plates $\varepsilon_1^0\ \mathbf{n}_1^0$ is also the in-plane minimal principal strain.

For thin plates, the bending strain changes linearly with the *z* value (Eq. 6) and only the bending strain at the top surface is calculated as

$$\varepsilon_1^1\ \mathbf{n}_1^1 = \varepsilon_1\ \mathbf{n}_1 - \varepsilon_1^0\ \mathbf{n}_1^0 \qquad (8)$$

where $\boldsymbol{\varepsilon_1 n_1}$ is the total minimal principal strain at the top surface and $\varepsilon_1^0\ \mathbf{n}_1^0$ is the in-plane minimal principal strain. Fig. 5 shows bending strains calculated based on Eq. 8. The regions within the dashed lines represent positive bending strain, while the rest of areas represent negative bending strains. The physical meaning of negative bending strain is that the top surface subject to more compressive strain than the middle. In the laser forming process operating under temperature gradient mechanism, the plate bends toward the laser beam. This indicates that the laser should be place on the top surface of the plate for this case. Since the positive bending strains are much smaller than the negative ones and occur in much smaller regions, and therefore are neglected in this case.

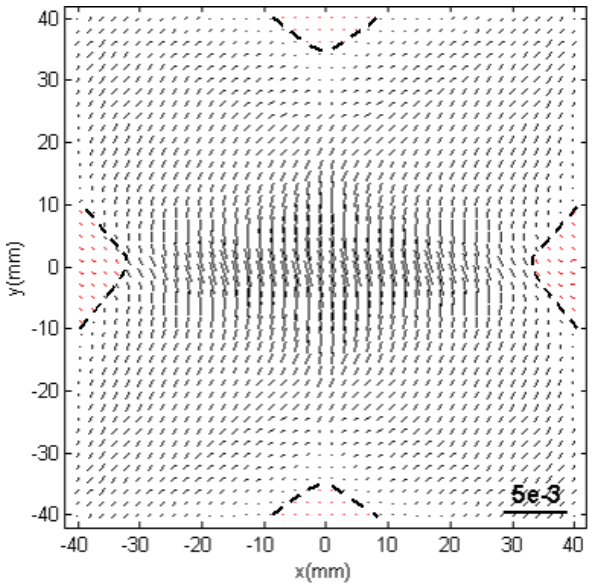

FIG. 5 VECTOR PLOT OF BENDING STRAIN OF THE PILLOW SHAPE (THE REGIONS WITHIN THE DASHED LINE ARE POSITIVE BENDING STRAINS)

Laser Forming FEM

After analyzing the strain field on the mechanical pressing side, the strain field in the laser forming process needs to be explored as well. In an effort to establish a database about the characteristics of laser forming induced strain distribution under various heating conditions, a simple straight line scanning along a centerline of a 80 by 80 by 1.4mm plate is assumed In the FEM simulation

of the laser forming process. Due to symmetry about the centerline, only half of the plate is simulated. The work piece material is assumed isotropic. Materials properties such as Young's modulus, yield stress, heat transfer properties, thermal conductivity and specific heat are temperature dependent. Material is 1010 steel. The heat flux of the laser beam is assumed to follow a Gaussian distribution. No melting is involved and no external forces are applied in the forming process. The symmetric plane is assumed to be adiabatic. Commercial FEM software, ABAQUS, is used to solve the thermal mechanical problem. Liu and Yao (2002) gives more details.

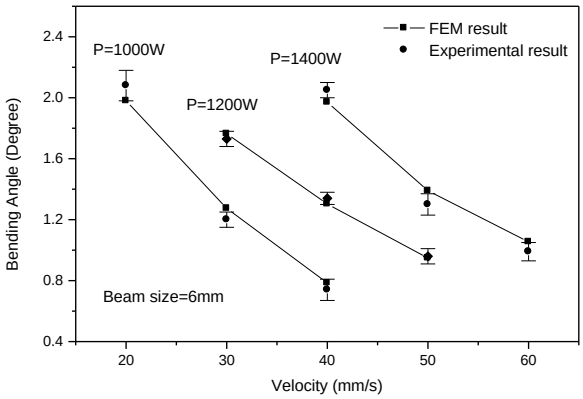

FIG. 6 EXPERIMENTAL VALIDATION OF NUMERICALLY DETERMINED BENDING ANGLE (THE ERROR BARS REPRESENT THE STANDARD DEVIATION OF TWO SAMPLES).

Fig. 6 shows a comparison of experimental and simulation results, the error bars represent the standard deviation from experiments. As seen from the plot, the bending angles calculated from FEM under various conditions are within the experimental errors. A database of in-plane and bending principal minimum strains under these conditions are established and the ratios between the in-plane and bending strains under these conditions are shown in Fig. 7. Obviously, many combinations of laser power *P* and scanning speed *V* are capable to give an identical ratio. This is indicative of the feasibility to choose a combination that matches not only the ratio but also the in-plane and bending strain values required by forming a desired shape indicated in the large-deformation elastic FEM.

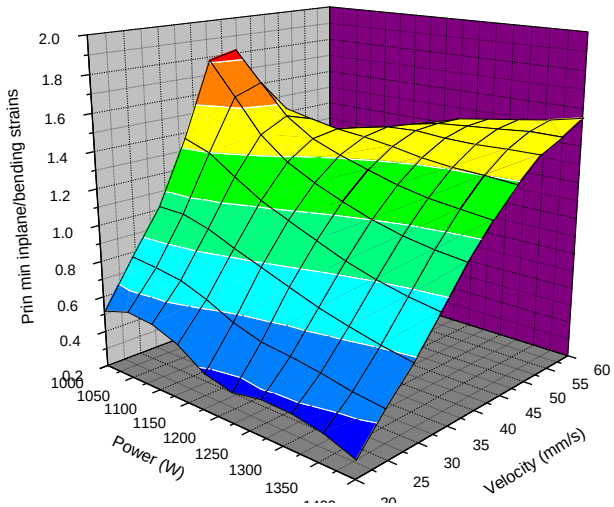

FIG. 7 FEM DETERMINED RATIO OF PRINCIPAL MINIMUM IN-PLANE STRAIN AND BENDING STRAINS (LASER BEAM DIAMETER IS 6MM).

SCANNING PATHS DETERMINATION

It has been discussed in the previous sections that the scanning paths should be placed perpendicular to the minimum principal strain direction because it is well known that the maximal compression occurs in the direction perpendicular to a laser scanning path in laser forming. For a very thin plate where bending strains are small, the in-plane minimal principal strain direction $\mathbf{n}_1^0$ should be used to determine the scanning paths. For the plate used in this study, there are sizable bending strains in some regions of the plate (Fig. 5), it seems more reasonable to average the in-plane strain direction $\mathbf{n}_1^0$ and the total strain direction $\mathbf{n}_1$ at the top surface, where the highest bending strain is found, as the basis for the laser path planning. Fig. 8 shows a quarter (due to symmetry) of the plate with averaged $\varepsilon_1^0\,\mathbf{n}_1^0$ and $\varepsilon_1\mathbf{n}_1$, which is used for scanning paths determination.

In determining the spacing of adjacent scanning paths, a number of guidelines are followed. In general, the smaller the spacing, the more precise the desired shape can be formed. Practically, however, the adjacent paths cannot be too close and also because being too close will violate the underlying assumption when using the laser forming FEM. The assumption is that adjacent paths should be independent with each other. The regions on a shape that have larger strains need to be scanned more and more exact

and therefore require denser paths. Roughly speaking, spacing between two adjacent paths, D_{paths}, should be equal to average strain generated by laser forming, ε_{laser}, multiplied by laser beam spot size, d_{laser} and divided by the average principal minimal strain over the spacing. Fig. 8 shows scanning paths determined following these guidelines. As seen, they are perpendicular to the minimal principal strain directions everywhere and denser around the center of the quarter due to larger strains there. Heating conditions are also indicated along the paths and their determination will be explained in the next section.

HEATING CONDITION DETERMINATION

If the laser spot size is given, the heating conditions to be determined include laser power *P* and scanning velocity *V*. While it is possible to continuously vary them to generate the strain field required to form the desired shape, this study adopts the strategy of constant power and piecewise constant speed for a given path in favor of implementation simplicity. The procedure is summarized below. A path is broken down to a few segments such that within each segment, the range of strain variation (highest minus lowest strain) is about the same as in other segments.

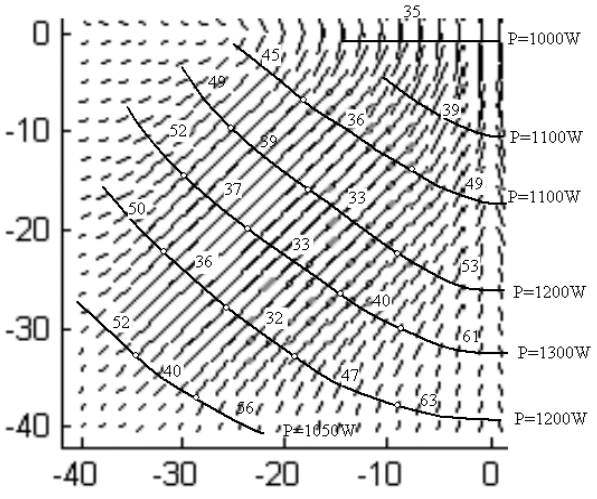

FIG. 8 LASER PATHS AND HEATING CONDITIONS DETERMINED FOR THE PILLOW SHAPE; ONLY QUARTER OF THE PLATE IS SHOWN DUE TO SYMMETRY; AND THE STRAIN FIELD SHOWN REPRESENTS THE MINIMAL PRINCIPAL IN-PLANE STRAIN AVERGED BETWEEN THE TOP AND MIDDLE SURFACES (THE NUMBERS NEXT TO THE SEGMETNS ON EACH SCANNING PATH REPRESENT SCANNING SPEED IN MM/S).

The segment having the largest strain, which has the strongest influence on the final shape, is first chosen. In determining the strain, strains between adjacent scanning paths are lumped together, because all these strains are to be imparted by the paths. The spacing of adjacent scanning paths is be determined by the lumped strains and the database. The highest and lowest in-plane minimal principal strains in the segment is averaged and compared with that from the database established by the laser forming FEM, resulting a group of (*P,V*) combinations. The process is repeated for the bending strains resulting another group of (*P,V*) combinations. The intersection of these two groups gives a unique (*P,V*) combination for the segment. The determined *P* value is also adopted for the entire path.

To determine scanning speed *V* for another segment on the path, a level of compromise is needed. Because, with *P* chosen, to find a *V* value which satisfies the required ratio of in-plane and bending minimal principal strains (using Fig. 5) as well as the strains themselves is generally unattainable. Assume V^0 and V^1 are the scanning speeds determined by the in-plane strain ε_1^0 and bending strain ε_1^1 from the database, the scanning speed for the segment is

$$V = \frac{\varepsilon_1^0}{\varepsilon_1^0 + \varepsilon_1^1} V^0 + \frac{\varepsilon_1^1}{\varepsilon_1^0 + \varepsilon_1^1} V^1 \qquad (9)$$

The procedure is repeated for other segments of the path as well as for all other paths. Fig. 8 shows the heating conditions determined following the above strategy. Due to symmetry, only one quarter of the plate is shown. As seen, a constant laser power is chosen for a path and a constant speed (unit: mm/s) for a segment.

EXPERIMENTAL VALIDATION

Experiments were conducted on 1010 steel coupons with dimension of 80 by 80 by 1.4 mm. The scanning paths and heating conditions in the experiments were determined as described above and indicated in Fig. 8. The laser system used is a PRC-1500 CO_2 laser, which is capable of delivering 1,500 W laser power and the laser beam diameter on the top surface of workpiece is 6mm. Motion of work pieces was controlled by Unidex MMI500 motion control system, which allows easy specifications of variable velocities along a path with smooth transitions from segment to segment.

Figure 9 shows the formed pillow shape under these conditions. A coordinate measuring machine (CMM) is used to measure the geometry of the formed shapes. The multi-scan simulation is not employed since comparison of the experiment result with the desired shape is more meaningful. Furthermore, the computation cost for multi-path simulation for the desired shape is so expensive that it beyond existing computing capacity. Figure 10 compares the geometry of formed shape under the determined conditions and the desired shape. Only the top

FIG. 9 LASER FORMED AISI1010 STEEL PLATES USING THE SCANNING PATHS AND HEATING CONDITIONS INDICATED IN FIG. 8.

surface of the plate is measured and compared. A general agreement can be seen from the figure and the middle of the plate shows some discrepancy. Possible sources contributing to the discrepancy include the lumped method used to sum strains between adjacent paths; finite number of paths to approximate a continuous strain field; and constant power for each path and constant velocity for each segment.

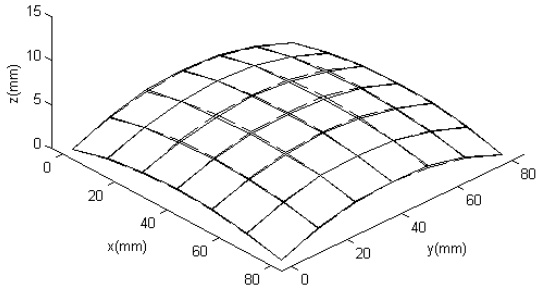

FIG. 10 COMPARISON OF FORMED SHAPE (SOLID LINES) AND DESIRED SHAPE (DASHED LINES). THE FORMED SHAPE WAS MEASURED BY CMM.

CONCLUSION

The FEM based 3D laser forming process design methodology for thin plates considering the effect of bending component are experimentally shown effective. A strain field required to form a desired doubly curved shape can be obtained through the large deformation elastic FEM independent of material properties. In determining heating conditions, the concept of in-plane and bending strain ratio is useful in approximately matching a strain distribution required to form a desired shape with that produced by a laser forming process.

ACKNOWLEDGEMENT

The work is supported in part by a NSF grant (DMI-0000081). Support from Columbia University is also gratefully acknowledged. Assistance in the large-deformation elastic FEM study provided by Prof. J. Cheng is greatly appreciated.

REFERENCES

Cheng, J., and Yao, Y.L., (2001), "Process synthesis of laser forming by Genetic Algorithms," Proceedings of ICALEO 2001, Section D 604.

Cheng and Yao, (2002), "Process Design of Laser Forming for Three-Dimensional Thin Plates," submitted to ASME J. of Manufacturing Science and Engineering.

Edwardson, S.P., Watkins, K.G., Dearden, G. and Magee, J., (2001), "3D Laser Forming of Saddle Shape", Proceedings of LANE 2001.

Liu, C. and Yao, Y.L., (2002), "Optimal and robust design of laser forming process," Journal of Manufacturing Processes, Vol. 4, No. 1, 2002.

Liu, C. and Yao., Y.L., Srinivasan.,V., (2002), "Optimal Process Planning for Laser Forming of Doubly Curved Shapes," Proceedings of ICALEO 2002.

Shimizu, H., (1997), "A heating process algorithm for metal forming by a moving heat source," M.S. Thesis, MIT.

Ueda, K., Murakawa, H., Rashwan, A. M, Okumoto, Y., and Kamichika, R., (1994a), "Development of computer-aided process planning system for plate bending by line heating (report 1) – relation between final form of plate and inherent strain," Journal of Ship Production, Vol.10 No.1, pp.59-67.

Ueda, K., Murakawa, H., Rashwan, A. M, Okumoto, Y., and Kamichika, R., (1994b), "Development of computer-aided process planning system for plate bending by line heating (report 2) – practice for plate bending in shipyard viewed from aspect of inherent strain," Journal of Ship Production, Vol. 10 No.4, pp.239-247.

Ventsel, E., and Krauthammer, T., (2001), "Thin Plates and Shells, Theory, Analysis and Applications," New York, Marcel Dekker, Inc.

Watkins, K. G., Edwardson, S. P., J. Magee, G. Dearden and P. French, (2001), “Laser Forming of Aerospace Alloys,” AeroSpace Manufacturing Technology Conference.